

Experimental investigation of nucleate boiling incipience with a highly-wetting dielectric fluid (R-113)

S. M. YOU, T. W. SIMON, A. BAR-COHEN and W. TONG

Department of Mechanical Engineering, University of Minnesota, Minneapolis, MN 55455, U.S.A.

(Received 21 October 1988 and in final form 16 May 1989)

Abstract—Experiments on pool boiling heat transfer in saturated R-113 at 1 atm pressure are conducted to investigate anomalies associated with the initiation of boiling using horizontal, 0.13 mm diameter chromel wires and a 0.51 mm diameter, platinum thin-film heater. Wall incipience superheat values of up to 73°C and wide variations in incipience superheats (more than 20°C) from case to case for nominally identical cases are observed. Presentation of incipience superheat results in terms of probability distributions is therefore recommended. The significant influence of the minimum heat flux and corresponding minimum wall superheat (after the cool-down portion of one run and the beginning of the subsequent run) on the incipience superheat excursion is observed. Tests with large step changes in heat flux, using a thin-film, cylindrical heater, indicated increases in incipience superheat of as much as 20% over tests with a series of incremental steps in heat flux up to the same heat flux level.

1. INTRODUCTION

THE HEAT flux of modern microelectronic chips has already exceeded one-twentieth that on the surface of the sun [1] and continues to increase with successive generations of devices. Innovative cooling schemes must therefore be implemented to maintain acceptably low junction temperatures as needed for reliable operation. Boiling heat transfer is being considered for these applications because it effectively cools the heated surface, showing small increases in surface temperature with large increases in power. Even though this has been realized for over 40 years [2], it has not been extensively used in the electronics industry. Recently, boiling of dielectric fluids was proposed as a promising cooling mechanism for future chips [1, 3]. However, concern over observed anomalies associated with the initiation of nucleate boiling was raised. These anomalies were discussed in detail in ref. [4]. Large superheat values were needed to initiate boiling when inert dielectric fluids proposed for computer cooling were used. This is of concern since a 15 ~ 20°C rise in junction temperature often doubles the chip failure rate [5].

Although the literature on boiling heat transfer is extensive, boiling behavior is not well documented for highly-wetting dielectric liquids like R-113 and FC-77 (Fluorinert used in the Cray-2). In the present study, pool boiling incipience of a highly-wetting liquid was investigated. R-113 was used as the working fluid and chromel wires as well as a platinum-coated quartz cylindrical heater were used as the boiling surfaces. This study presents means and variations about the

means, of incipience superheats and thermal excursions, based upon multiple-run cases. As far as the authors know, this is the first time that incipience data have been presented in this format.

1.1. Previous work

Corty and Foust [6] and Bankoff *et al.* [7] were among the first investigators to observe the wall temperature excursion at the beginning of nucleate boiling. These and other experimental results (published prior to 1986) on incipience wall superheat excursions were discussed in ref. [4]. These results, listed in Table 1, showed significant variations from case to case. Possible mechanisms for delayed nucleation were discussed and approximate methods presented for calculating superheat excursions at incipience in ref. [4].

Danielson *et al.* [8] conducted saturated pool boiling experiments with a 0.25 mm platinum wire heating element using several inert liquids (FC series and R-113). Based on their observations, superheat excursions at boiling incipience differ widely from case to case even for the same fluid and wire. In a study by Berenson [9], nucleate boiling heat transfer coefficients varied by 600% due to variations in surface finish. He strongly emphasized the importance of the surface roughness—a rougher surface, in the boiling sense, is one which has a greater number of cavities of appropriate size, regardless of the more traditional r.m.s. roughness definition. Recent investigations on surface effects in pool boiling by Chowdhury and Winterton [10] confirmed that an increased number of active

NOMENCLATURE

C	specific heat
g	gravitational acceleration
h	enthalpy
P	pressure
ΔP	pressure difference across bubble interface
Pr	Prandtl number
q/A	heat flux
r_b	embryonic bubble radius inside cavity
r_c	radius of cavity mouth
T	temperature
ΔT_{ex}	superheat excursion
ΔT_s	superheat needed at the onset of nucleate boiling
v	specific volume.

Greek symbols	
β	contact angle
μ	dynamic viscosity
ρ	density
σ	surface tension.

Subscripts

c	thermodynamic critical condition
fg	liquid/vapor transition
h	homogeneous nucleation
l	liquid
sat	saturation
v	vapor
w	wall.

nucleation sites moves the nucleate boiling curve toward lower wall superheats. From their observation, nucleate boiling heat transfer appears to be unaffected by contact angle.

Kozawa *et al.* [11] conducted boiling experiments with R-113 and copper foil heater surfaces fabricated with different densities of hour-glass-shaped pinholes and found a 5°C decrease of superheat in the fully developed nucleate boiling regime due to the holes. While the smooth surface experienced about 30°C superheat excursion, the excursion vanished when the pinhole surface was used. Venart *et al.* [12] compared boiling with R-11 on non-porous and two surfaces with porous coatings finding that the enhanced (porous) surfaces showed decreases in nucleate boiling superheat. However, the incipience wall superheat values for the three different surfaces were similar. Therefore, increases in the temperature excursion were observed for the porous surfaces.

1.2. Some theoretical background on boiling incipience

Griffith and Wallis [13] presented a criterion for predicting vapor superheat required to initiate boiling as

$$\Delta T_s = T_w - T_{sat}(P_1) \cong \Delta P(dT/dP)_{sat} = (2\sigma/r_b)(dT/dP)_{sat} \quad (1)$$

where $r_b = r_c$, the cavity radius. Here, using the Clausius-Clapeyron equation, $(dT/dP)_{sat}$ can be estimated as

$$(dT/dP)_{sat} \cong [T_{sat}(P_1)v_{fg}]/h_{fg}. \quad (2)$$

This prediction is appropriate when the contact angle is large ($\sim 90^\circ$), the incipience superheat is small and the saturation curve is nearly linear over the range from the saturation temperature of the liquid to the temperature of the superheated vapor within the bubble.

Table 1. Incipience wall superheat excursions

Authors	ΔT_{ex}	Working fluid	Surface
Bergles <i>et al.</i> (1968)	15–27°C	R-113	S.S. tubing
Seeley and Chu (1972)	12°C	R-11	Ferrite cores
Murphy and Bergles (1972)	10–14°C	R-113	S.S. tubing
Nghiem <i>et al.</i> (1980)	30°C	R-113	Thin gold film
Reeber and Frieser (1980)	no nucleation (for $\Delta T_s < 46^\circ\text{C}$) 8°C	FC-72	Polished silicon
		FC-72	Etched gold film
			Eutectic surface
Oktaç (1982)	23°C	FC-86	Plain Si chip
	15°C	FC-86	Sandblasted/KOH treated chip
Moran <i>et al.</i> (1982)	20°C	FC-86	Without surface finish
	30°C	FC-86	With surface finish
Giarrantano (1984)	20°C	Liquid nitrogen	Thin platinum film
Ogiso (1985)	several degrees	Liquid nitrogen	Silicon chip
Samant and Simon (1986)	$\sim 40^\circ\text{C}$	FC-72	Thin nichrome film
Present study	10–23°C	R-113	Chromel wire
	29–53°C	R-113	Thin Pt film

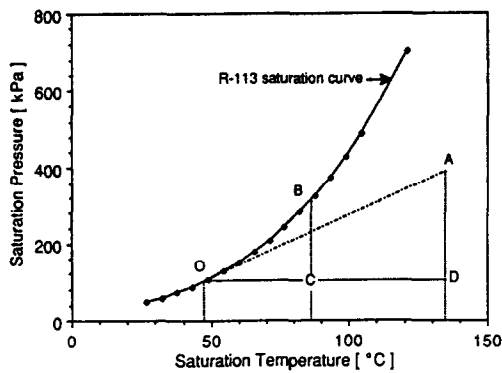


FIG. 1. Boiling incipience prediction with R-113 saturation curve.

As discussed by Bar-Cohen and Simon [4], Marsh and Mudawwar [14], Lorenz *et al.* [15] and Tong *et al.* [16] the incipience mechanism for highly-wetting fluids may be different from that of poorly-wetting fluids. Some important differences are as follows. (1) On a given surface, there will be a larger number of active embryos (gas retained in cavities) with poorly-wetting liquids (e.g. water) than with highly-wetting liquids (e.g. dielectric fluids). This is due to the enhanced ability of fluids of small wetting angle to effectively flood the cavities. (2) The residual bubble in highly-wetting liquids is small and represents the configuration of minimum radius of curvature in its eventual growth ($r_b < r_c$). Initial growth from this stage therefore requires the maximum superheat of the bubble's life. (3) Because of this larger incipience superheat, a nonlinearity of the saturation curve may result in a significant error in superheat computed from equations (1) and (2). An equivalent expression for computation of the incipience superheat in highly-wetting fluids, is

$$\Delta T_s = T_w - T_{\text{sat}}(P_1) \cong T_{\text{sat}}(P_1 + 2\sigma(T_w)/r_b) - T_{\text{sat}}(P_1) \quad (3)$$

Here, r_b is the radius of the embryonic bubble which, for the highly-wetting fluids, will be smaller than the cavity mouth radius, r_c [16]. Equation (3), with surface tension values evaluated at T_w , is utilized in this paper to estimate the embryonic bubble radius from measured incipience superheat values.

The boiling incipience prediction is illustrated using the saturation curve for R-113 in Fig. 1. The wall superheat required to maintain a $0.1 \mu\text{m}$ radius, embryonic bubble of R-113 vapor in a liquid at atmospheric pressure is computed from equations (1) and (3). With the assumptions of equation (1) the computed pressure difference AD yields a superheat, OD, of 87°C . Using equation (3) the computed pressure difference BC yields a superheat, OC, of 39°C . The two computed pressure differences are not the same partially because in equation (3) the surface tension is based upon the wall temperature whereas in equation (1) it is based upon the saturation temperature

of the liquid. The largest difference between the two computed superheat values, however, comes from the nonlinearity of the saturation curve over this pressure difference.

The incipience superheat is bounded from above by homogeneous nucleation as discussed in ref. [4]. This is the nucleation mechanism which will come into play in the absence of sufficiently large embryonic bubbles on the heated surface. This limiting superheat can be estimated using a correlation proposed by Lienhard [17]

$$\Delta T_{\text{homogeneous}} = T_h - T_{\text{sat}} = T_c [0.923 - (T_{\text{sat}}/T_c) + 0.077(T_{\text{sat}}/T_c)^9] \quad (4)$$

Equation (4) is used as the upper limit of the incipience superheat for comparison with experimental data. No cases were found in the present study where this upper limit was reached.

2. EXPERIMENTAL APPARATUS

A 1 kW immersion circulator/heater, a 1 kW immersion heater and a 300 W bath cooling unit provided a uniform and constant temperature for the 32 liter glass container, in which the test vessel was immersed. The test vessel was a 2 liter glass container in which the test fluid and heating element resided. The test fluid temperature, measured by copper-constantan thermocouples and by a platinum RTD sensor, remained constant and uniform to within 0.05°C .

The facility was controlled and monitored with a small laboratory computer that interfaced with a 30-channel data acquisition/control unit and a d.c. power supply programmer via IEEE-488 interface cables. Direct current was supplied to the heating element and a series precision resistor by a power supply. Separate voltage taps across the heating element and across the precision resistor were used to compute heater resistance and heating element power. Heating element temperature was computed from its resistance via a calibration curve taken before the experiment. Computed temperatures and heat fluxes were averages of 20 samples taken over a 50 s period.

The present investigation was conducted with saturated R-113 fluid under atmospheric pressure and electrically-heated 0.13 mm diameter chromel wires (90% nickel) and with a 0.51 mm diameter cylindrical heater. The second heater was constructed with a thin platinum film on a quartz rod. The heated areas of the two heaters were 0.36 and 0.41 cm^2 , respectively. The saturation temperature of the R-113 was determined by the total pressure and the dissolved gas content. Measurements with a Seaton-Wilson Aire-Ometer indicated that the dissolved gas content, on a volume basis, for all tests, was essentially zero (0–1.0%)—a 1% by volume dissolved gas content will change the saturation temperature only 0.5°C . As

a point of reference, R-113 saturated with air at 25°C and 1 atm has a 40% volumetric air fraction.

The chromel wires were cut from commercially available thermocouple wires. The nominal measured resistance was 4.8 Ω and the calibration slope was $572 \pm 6^\circ\text{C } \Omega^{-1}$. The thin-film heater, 25.4 mm long and 0.51 mm in diameter, was made by sputtering a film ($\approx 0.1 \mu\text{m}$) of platinum on a quartz cylinder. Its resistance was 20 Ω and its calibration slope was $24.0^\circ\text{C } \Omega^{-1}$, within 1%. Both heaters displayed a linear relationship between temperature and resistance and, therefore, could serve as both heaters and wall temperature sensing devices. The large aspect ratios of the heaters resulted in minimal conduction losses and nearly-uniform heat flux.

2.1. Qualification of the test facility

Analyses were performed for evaluating uncertainties of heat fluxes and wall superheats (differences between the heating element temperatures and the saturated pool temperatures) under various regimes of boiling. The techniques of Kline and McClintock [18] were used to compute the propagation of uncertainties. The computed uncertainty of heat flux was 2% and that of the wall superheat was 0.7°C for all but a few points near the incipience of nucleate boiling, at which 1°C was assigned. The increase in uncertainty of wall superheat near incipience was due to the larger unsteadiness at this rather unstable location.

When a heating element immersed in a pool of quiescent liquid is electrically heated, a buoyancy-induced motion due to density gradients generates natural convection flow. This is the operative mechanism for a portion of the test, labeled 'single-phase convection' on the 'boiling' curves to be presented. Experimental results were compared with a correlation recommended by Kuehn and Goldstein [19]. Measurements (not shown) agreed within 5% for Rayleigh numbers from 1 to 10000. The close agreement lent confidence to the test procedure.

3. RESULTS AND DISCUSSION

3.1. Saturated pool boiling experiments with a chromel wire

A typical single-run boiling curve, heat flux vs wall superheat, is shown in Fig. 2. Distinct single-phase and nucleate boiling regimes are observed, when the heat flux increased in small steps, with an abrupt temperature decrease of about 15°C when the single-phase curve reaches 28°C superheat. In the present study, the superheat excursion at the incipience of nucleate boiling is defined as the maximum temperature difference (along a line of constant heat flux) between the surface temperature for increasing heat flux and that for decreasing heat flux. The lengths of the horizontal bands in Fig. 2 indicate the magnitude of two-standard-deviation intervals computed from 20 readings taken over a 50 s period at a constant heat flux. They, thus, are indicators of unsteadiness. This

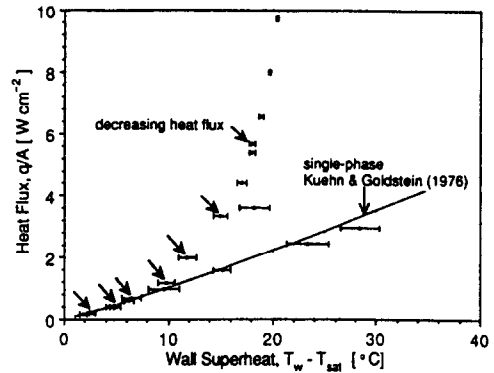


FIG. 2. Unsteadiness of saturated pool boiling (R-113, first chromel wire).

unsteadiness is shown to peak in the vicinity of boiling incipience, with a two-standard-deviation value of $\sim 2^\circ\text{C}$.

Results of ten consecutive runs, each with heat flux incrementally increasing to the maximum value of the test then decreasing to zero, are shown in Fig. 3. These runs were computer-controlled to step through precisely the same heat flux conditions (each starting from zero heat flux). Note that this repeatability test is quite different from the unsteadiness test recorded in Fig. 2. Large non-repeatability values from case to case appeared in the region of onset of nucleate boiling. The highest heat flux attainable in the natural convection regime prior to boiling varied from 2.4 to 4.4 W cm^{-2} for the ten runs. The maximum excursion of the ten runs was about 23°C. The order in which the ten runs were taken is given by the run numbers. Note that the curve shapes are random; there is no discernible trend in the incipience behavior with run number. The averaged values and the two-standard-deviation ranges of temperature for the ten runs of Fig. 3 are shown in Fig. 4. The repeatability is clearly good for much of the curve while poor (a maximum standard deviation of 8°C) in the vicinity of boiling incipience. The data suggest that incipience of nucleate boiling of highly-wetting liquids may be better displayed by statistical or probabilistic means.

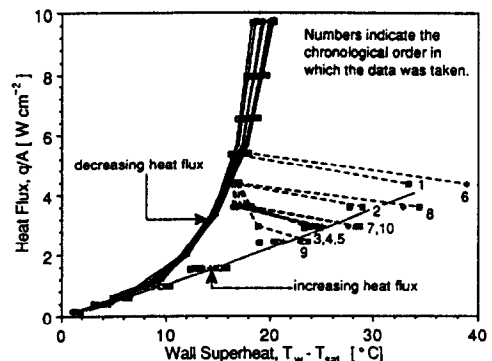


FIG. 3. Pool boiling runs (R-113, first chromel wire).

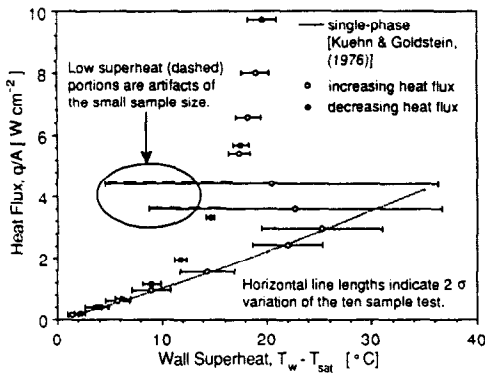


FIG. 4. Repeatability of ten pool boiling runs (R-113, first chromel wire).

Figure 5 shows a probability distribution that does so. Here, the probability of boiling incipience is plotted vs the value of single-phase, natural convection, wall superheat. As shown, all cases reached 23°C superheat without boiling (0%). The last case to boil did so at 39°C and 50% of the cases had begun boiling before a single-phase wall superheat of 26.5°C was reached. Throughout the ten test runs, transition from single-phase natural convection to nucleate boiling was accompanied by the appearance of columns of bubbles. This transition was more abrupt and many more bubble columns were immediately formed (the surface temperature therefore abruptly dropped) when higher incipience superheat values were attained. A more gradual transition from single-phase natural convection to fully-developed nucleate boiling, allowing opportunities to measure intermediate points, was observed for cases of smaller incipience superheat values (see curve 9 of Fig. 3). It appeared that the locations, on the heater surface, of the initial bubble columns for the ten different curves were random; there was no repeated or consistent trend in the behavior from one run to the next.

From the large unsteadiness (Fig. 2) and the poor repeatability (Figs. 3 and 4), the onset of saturated nucleate boiling is apparently a very unstable process.

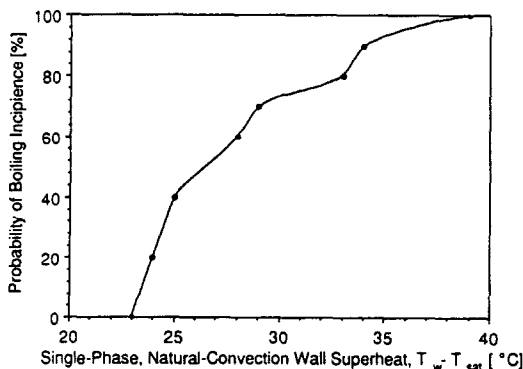


FIG. 5. Probability of boiling incipience vs single-phase, natural-convection wall superheat: obtained from ten consecutive runs (R-113, first chromel wire).

Such unstable behavior may be attributed to both the good wetting characteristics and the poor reproducibility of contact angle from case to case; a discussion of this follows. First, only a few cavities are candidates for trapping gases when the wetting angle, β , is small. When few cavities participate, the results can change considerably if candidate cavities are sometimes active and sometimes inactive. This introduces a sensitivity to changes in wetting angle. This sensitivity and the difficulties of contact angle measurement were reported in the following literature. Contact angle measurements for water on clean stainless steel surfaces indicate a very wide distribution in values from 30° to 90° [13]. The contact angle of R-113 with polished copper was reported to be near zero [20]. One may therefore imagine large variations of its value, expressed as a fraction, with small changes in fluid and surface conditions; although this has not been experimentally verified. Movement of the triple (liquid/vapor/solid phases) contact line on a solid surface is expected throughout the boiling phase of the experiment. Schwartz and Tejada [21], employing hexadecane on a stainless steel surface, found that the contact angle increased linearly from $\sim 0^\circ$ to 25° depending on the velocity between 0.2 and 10 mm s⁻¹. Movement of the contact point can thus result in a velocity-dependent and position-dependent contact angle. This may change the trapping of gases for bubble embryos, and thus, the boiling incipience superheat in a random manner.

Equation (3) was used to determine the effective embryonic bubble radius in each of the above ten runs; values ranged from 0.10 to 0.23 μm . The smallest radius, 0.10 μm , corresponded with the highest wall superheat value of 38.9°C. Since the measured superheat values were substantially below the homogeneous nucleation superheat values computed from equation (4) (130°C in this case), it appears that heterogeneous nucleation was the operative nucleation mechanism for all the cases.

3.2. Experiments with a second chromel wire

An ostensibly identical test was conducted with a second cut of chromel wire which was taken from the same manufactured run of wire as the first. The boiling curve taken with this wire lies further to the right than does that of the previous wire. Following Rohsenow [22], nucleate boiling curves may be correlated as

$$\frac{C_1(T_w - T_{\text{sat}})}{h_{\text{fg}}} = C_{\text{sf}} \left\{ \frac{q/A}{\mu_l h_{\text{fg}}} \sqrt{\left(\frac{\sigma}{g(\rho_l - \rho_v)} \right)} \right\}^b Pr_l^a \quad (5)$$

Here, the recommended value of b for R-113 is 1.7. For the second chromel wire, a different C_{sf} value (0.0063 compared to 0.0040 for the first wire) and a different constant, a (0.165 compared to 0.208 for the first wire), were found. According to Rohsenow [22], C_{sf} has been found to range from 0.0025 to 0.015. The differences in C_{sf} and a for these two wires are presumed to be due to different distributions of cavi-

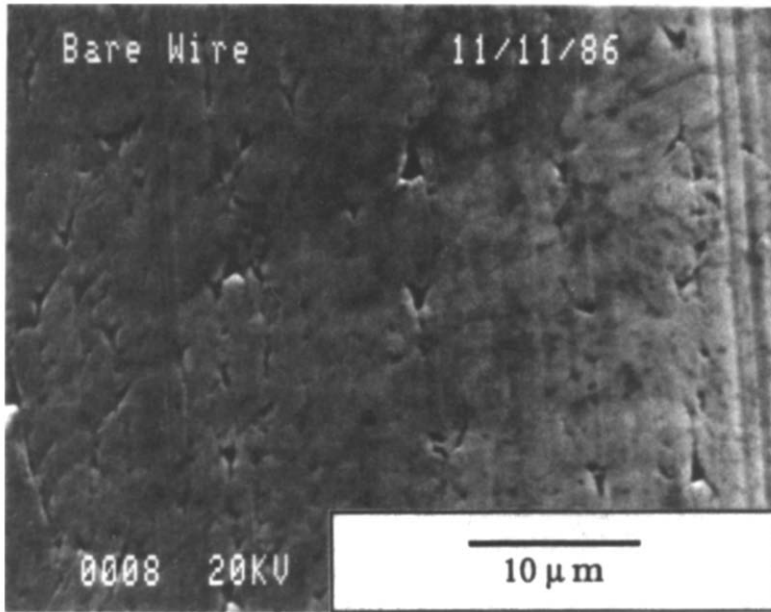


FIG. 6. Surface micro-geometry taken by SEM—sample chromel wire ($\times 2500$).

ties for the two heating elements, even though they were cut from the same manufacturing run. These differences may be due to variabilities during the manufacturing processes, e.g. die chatter. Danielson *et al.* [8] reported C_d and a values for a 0.25 mm platinum wire in saturated R-113 of 0.005 and 0.17, respectively. Though the nucleate boiling curves for the two chromel wires discussed above were different, predicted embryonic bubble diameters for the second wire, corresponding to the measured incipience superheats, were within the range of the first wire; $0.10 \sim 0.23 \mu\text{m}$.

After the experiments, the surface geometry of the second chromel wire was examined using a scanning electron microscope (SEM) and compared with another sample wire from the same run (see Figs. 6 and 7). Both surfaces showed many pits of various sizes up to an equivalent diameter of $2 \mu\text{m}$. These pits may have been caused during the extrusion process—many axially-oriented scratches can be observed. It appears from Fig. 7 that it is likely that many cavities of the $0.1 \sim 0.2 \mu\text{m}$ size range exist. Also, many pits associated with deep cracks (possibly due to thermal stress cracking) were found; thus, the included angle of such pits may be small. Such small-angle pits could be expected to enhance the trapping process.

3.3. Experiments with different starting conditions using the second chromel wire

The effect of varying the minimum heat flux (the beginning heat flux of the heat-up portion of each cycle and the minimum heat flux ending the cool-down portion of each cycle) was next investigated. In these tests, the heat flux was incrementally decreased after establishing nucleate boiling at 10.4 W cm^{-2} ,

continuing until a specific, non-zero minimum heat flux was reached. This minimum heat flux was maintained for about 1 min. Then, without decreasing the power, a heat-up cycle with incremental, stepwise-increasing heat flux changes was begun and the boiling behavior was documented. Each heat-up cycle was concluded and the ensuing cool-down cycle was begun when a heat flux of 3.66 W cm^{-2} was reached. Minimum heat flux values for successive cases were 2.10, 1.05, 0.727 and 0.158 W cm^{-2} for cases 1, 2, 3 and 4 of Fig. 8, respectively. Corresponding minimum wall superheat values were 15, 9.5, 7, and 2.2 C . No bubble column was observed at minimum heat flux values of the 0.727 and 0.158 W cm^{-2} cases. Tests were repeated ten times for each particular minimum heat flux value. Average values and two-standard-deviation intervals for each ten-run series are shown on Fig. 8. Case 1 was entirely within the nucleate boiling regime and case 4 was entirely within the single-phase natural convection regime. As the minimum heat flux (or starting heat flux for the test) decreased from that of case 1 (2.10 W cm^{-2}), the superheat value ($T_w - T_{\text{sat}}$) at the maximum heat flux of each run, 3.66 W cm^{-2} , increased from the nucleate boiling value (case 1 of Fig. 8) to the largest single-phase natural convection value (case 4). A trend showing a consistently decreasing number of bubble columns at the maximum heat flux (many, 4, 2 and 0 columns, for cases 1, 2, 3 and 4, respectively) was observed.

For cases 3 and 4 (superheat of 7 and 2.2 C at the minimum heat fluxes, respectively), no bubble column was seen at the start of the run. As the heat flux was increased to 3.66 W cm^{-2} , case 3 showed two columns of bubbles whereas case 4 showed no bubbles. This may be due to larger embryonic bubbles inside the

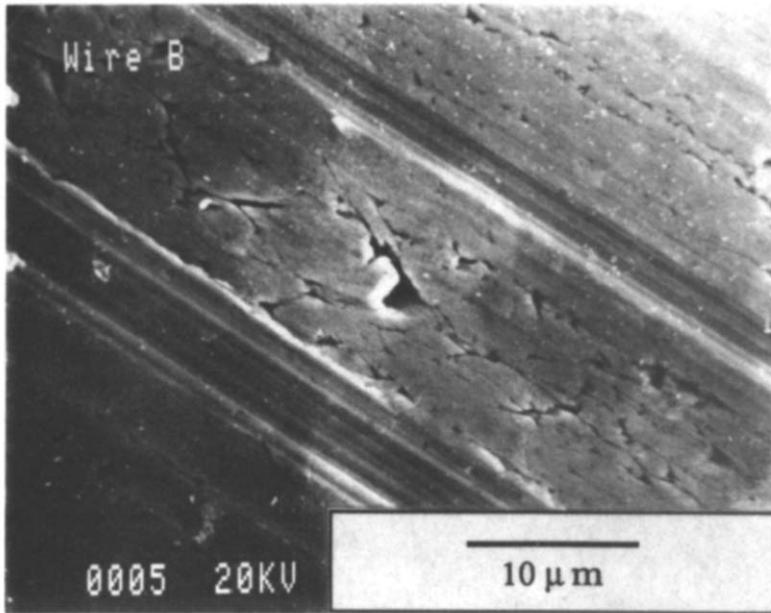


FIG. 7. Surface micro-geometry taken by SEM—second chromel wire ($\times 2500$).

cavities at the beginning of the heat-up cycle for the higher initial heat flux case (case 3) requiring a lower superheat to activate nucleation than for the embryonic bubbles of the lower initial heat flux case (case 4). This scenario is consistent with the hypothesis presented by Lorenz *et al.* [15] and Tong *et al.* [16] (see Fig. 3 of ref. [16]) that, for highly-wetting fluids, the minimum radius of bubble embryos is attained within the cavity and not at the mouth of the cavity. If the minimum radii of bubbles curvature were experienced when the bubble were at the mouths of the cavities, both cases 3 and 4 (which appeared to be the same at the minimum heat fluxes) would have displayed similar incipience behavior.

3.4. Saturated pool boiling experiments with the thin-film heater

The thin-film heater constructed with a sputtered platinum surface on a quartz cylinder was next intro-

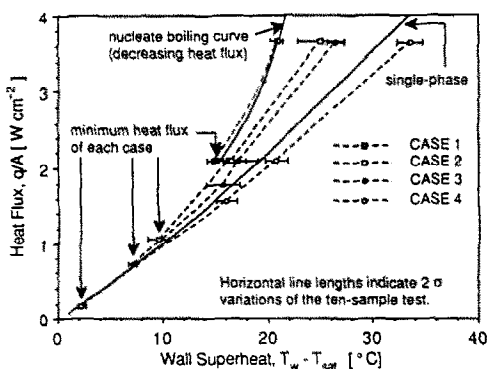


FIG. 8. The effect of varying minimum heat flux at the beginning of the heat-up cycle (R-113, second chromel wire).

duced to further investigate the effects of surface characteristics on the initiation of nucleate boiling and on the nucleate boiling curve. The test program was precisely the same as with the wires—only the heating element was replaced. Before examining the nucleate boiling characteristics, the surface micro-geometry was documented using SEM. A portion of the platinum film containing a large cavity and a number of smaller cavities is shown in Fig. 9. There were no other large cavities, like the one shown, found during the SEM scan (although there may have been others outside the scanning field of view); the remainder of the coated cylinder appeared more like the left-hand portion of Fig. 9. This obviously differed from the surface geometry of the chromel wire shown in Fig. 7—it was much smoother and had much fewer large cavities.

During operation, the thin-film heating element became coated with dark deposits (shown in Figs. 10 and 11) during each set of runs. These were similar in appearance to deposits reported by Akagawa *et al.* [23]. They found that a 0.29 mm platinum wire heater in R-11 or R-113 was contaminated with deposits. It was presumed that the deposits were formed with products of thermal decomposition of the fluid under film boiling. They noted that no fouling deposit occurred for surface temperatures below 100°C. In a film boiling study of R-113 by Yilmaz and Westwater [24], dark deposits were seen when wall temperatures exceeded 170°C. In the present study, the formation of deposits was not observed in the chromel wire cases, in which the maximum wall temperatures were less than 80°C, but deposits were observed with the platinum film heater when temperatures exceeded 100°C. In successive data runs performed immediately after each cleaning of the surface with an ultra-sonic bath of

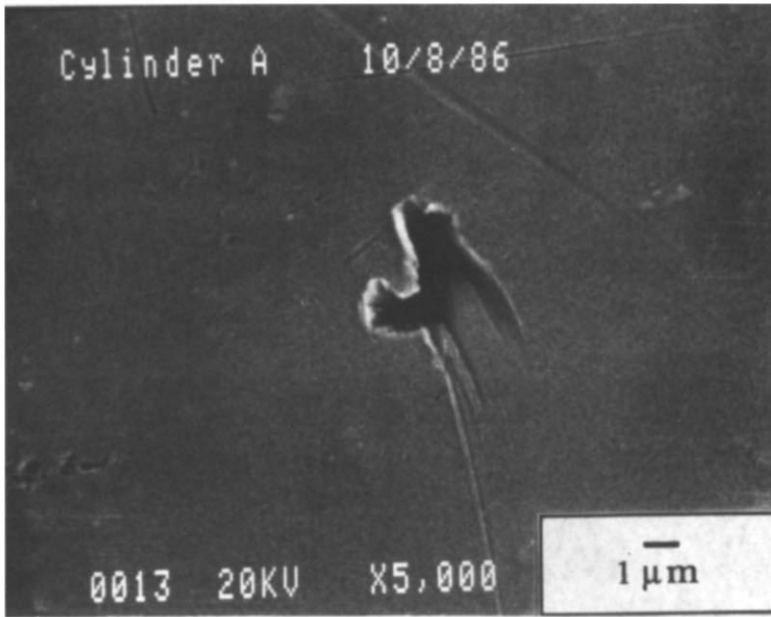


FIG. 9. Surface micro-geometry taken by SEM—Pt thin-film heater ($\times 5000$).

acetone, wall superheat values in the nucleate boiling regime decreased progressively as a result, it is presumed, of the growing deposits. No changes in the natural convection portions of the curves due to this contamination were observed. Eventually, within ten runs after each cleaning, repeatable boiling curves were achieved (see Fig. 12). SEM pictures taken after these ten runs show the fouling deposits (see Figs. 10 and 11). The high superheat ($>100^\circ\text{C}$) required to

initiate nucleate boiling of a highly-wetting liquid on the smooth platinum-sputtered surface is presumed to cause fluid decomposition leading to the creation of fouling deposits and the corresponding changes in the nucleate boiling curve. Therefore, in order to conduct a series of consistent tests, the surface contamination was allowed to continue until no more change in wall superheat was observed. This surface was then used for the remainder of the runs discussed herein. Before

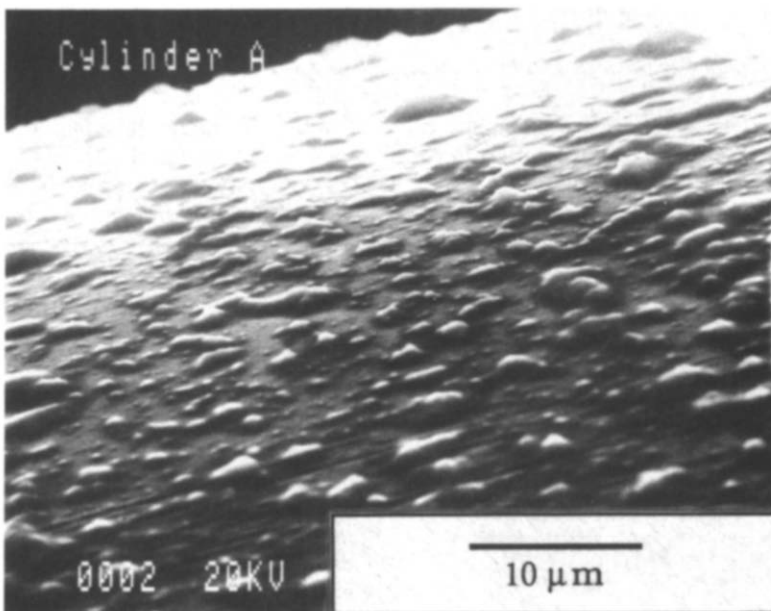


FIG. 10. Pt thin-film heater coated with dark deposits ($\times 2500$).

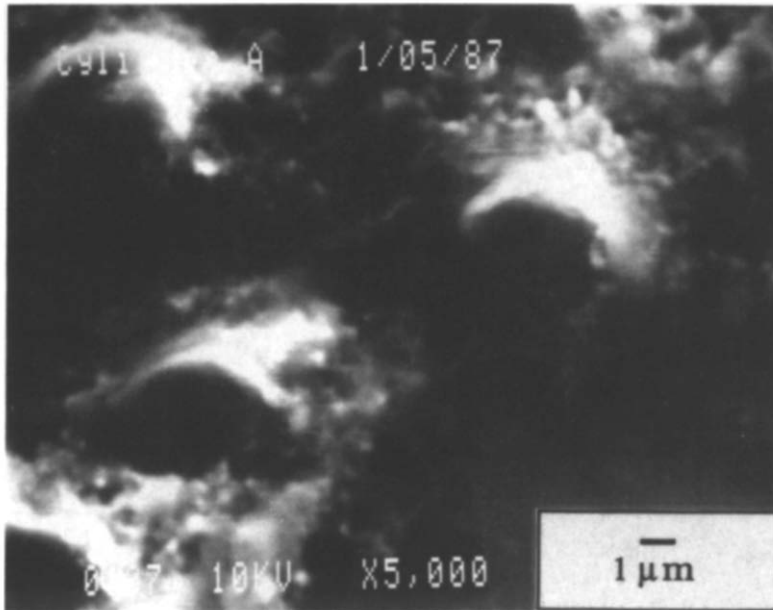


FIG. 11. Pt thin-film heater coated with dark deposits ($\times 5000$).

discussing these runs, the following observations about the effect of the deposits are noted. Even though a dramatic change in surface micro-geometry can be seen (Figs. 9–11), no significant change in the incipience superheat was observed in the data. There was a decrease in nucleate boiling superheat values, however. This implies that there was no significant effect of the fouling deposits on those cavities which were activated upon initiation of boiling ($\sim 0.02\text{--}0.06\ \mu\text{m}$ range), but the deposits shown in Fig. 11 provided more bubble nucleation sites for fully-developed boiling (cavity sizes in the $0.2\ \mu\text{m}$ range).

Fifteen consecutive runs with increasing, then decreasing, heat flux values were next performed, using R-113 at 1 atm pressure and the ‘contaminated’ surface shown in Fig. 11. The results are shown in Fig. 13. Again, single-phase data agreed with the correlation of Kuehn and Goldstein [19]. The maximum excursion was about 53°C and the wall incipience

superheats of these runs ranged from 49.1 to 72.5°C (recall that the maximum excursion attained for the wire tests was $23\ \text{C}$ and the highest superheat was 38.9°C). This comparison was expected, based on the different surface micro-geometries—the wire surfaces (e.g. Fig. 7) appeared to have many pits or cavities of submicrometer sizes with, it is presumed, small cavity angles; but, the thin-film heater (Figs. 10 and 11) was much smoother. The behavior following the first appearance of boiling was also markedly different for the thin-film heater. For all these tests, the wall superheat values returned abruptly to the fully-developed nucleate boiling range when the heat flux was increased incrementally beyond the maximum single-phase value. During this increment, bubble columns formed immediately across the entire heating element—recall the stepwise transition from single-phase natural convection to fully-developed nucleate boiling experienced in many of the runs in which the

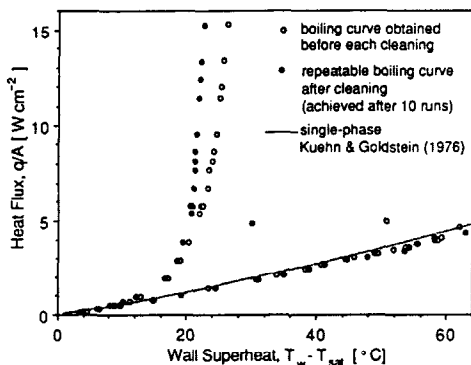


FIG. 12. The effect of fouling deposits on boiling curve—Pt thin-film heater.

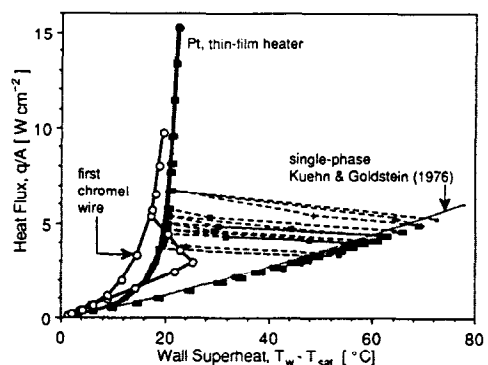


FIG. 13. Pool boiling runs (R-113, Pt thin-film heater and first chromel wire).

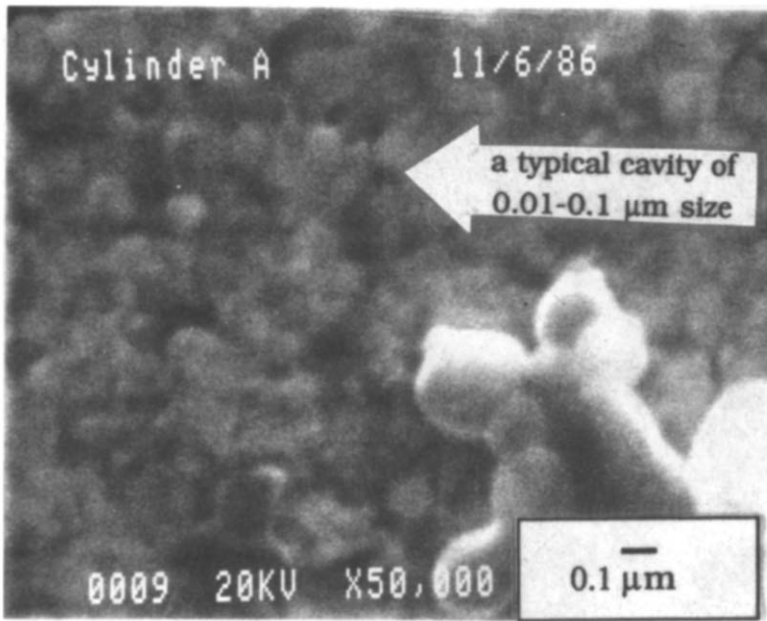


FIG. 14. Pt thin-film heater surface ($\times 50\,000$).

drawn wire was used as the heated surface (e.g. Run 9 of Fig. 3).

Effective incipience bubble radii, r_b , for the 15 runs on the platinum film heater were computed with equation (3). They ranged from 0.023 to $0.062\ \mu\text{m}$, substantially smaller values than those for the wire (0.10 – $0.23\ \mu\text{m}$). A highly-enlarged SEM picture of the thin-film surface (Fig. 14) shows the structure of the sputtered platinum film. This figure seems to indicate many cavities between 0.01 and $0.1\ \mu\text{m}$, a range which corresponds to the r_b values which were computed from the measured incipience superheat values. These cavities, it is felt, are those which serve as active sites for boiling incipience. Higher nucleate boiling superheat values were observed for this thin-film heater surface than those observed with the drawn wires (Fig. 13). This also is presumed to be due to the smoother surface. Differences, between the wire and platinum film cases, in fully-developed nucleate boiling superheat are much smaller than those at incipience, however.

The probability of experiencing boiling incipience vs single-phase, natural convection wall superheat, for the thin-film heater, is plotted in Fig. 15. All cases reached 48°C superheat without boiling (0% probability), and, at 72°C , the last case boiled (100% probability). A comparison of the two surfaces at equal probability points shows that the incipience superheat for the sputtered surface is approximately two times that for the drawn-wire heater.

3.5. Tests with large steps in heat flux using the thin-film heater

In the experiments discussed thus far, the boiling curves were generated by taking incremental steps up or down in heat flux, allowing sufficient time to

achieve steady state, then sampling over a 50 s period. Simulating the turning-on transients of electronic equipment, the next series of tests were carried out by introducing a large step in heat flux, from zero to various test heat flux levels. The average of 20 samples for each particular level of heat flux was then measured. Data was not recorded until steady-state heater temperatures were reached, sometimes requiring as long as 2 min (less than $50\ \mu\text{s}$ were required for the step change in heat flux). The curve for probability of boiling incipience (Fig. 15) for this large-step test was next calculated using 20 repeated runs. The purpose of this test was to see the effect of a large step in heating on the probability curve. As shown, the magnitudes of the wall superheats for this test lie as much as 20% above those for the test with small, incremental increases in heat flux. Though no explanation is proposed at this time, observations from this test appear to be consistent with those from a transient

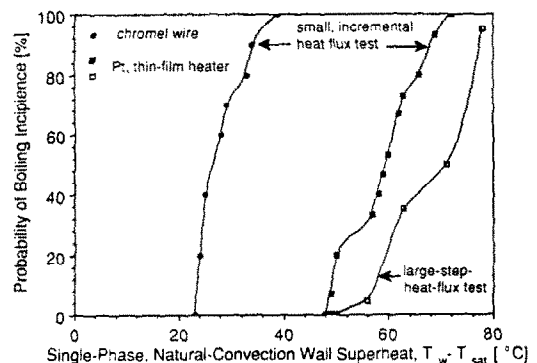


FIG. 15. Probability of boiling incipience vs single-phase, natural-convection wall superheat.

boiling incipience study by Nghiem *et al.* [25]. In a test where the heat flux was increased abruptly from zero to a specified value and the transient temperature response was recorded, Nghiem *et al.* observed higher superheat for the transient boiling incipience at progressively higher values of the specified heat flux. The incremental heating tests of the present study, characterized by small steps of heat flux and allowance of sufficient time at each value to achieve a steady state, took 20–50 min to arrive at the measurement conditions, while the large-step tests took about 50 μ s to achieve the desired heat flux and, at most, 2 min to arrive at a steady state. Therefore, the two thin-film heater probability curves in Fig. 15 seem to serve as limiting cases for the upper and lower bounds on incipience wall superheat after achieving a steady state with this heater, but with different heat flux vs time trajectories. The two probability curves, therefore, indicate the range of heat flux values or superheat values one might expect to be required for the boiling incipience, regardless of how the heater was powered.

4. SUMMARY AND CONCLUSIONS

The thermal excursion at the onset of nucleate boiling was investigated using horizontal 0.13 mm chromel wires and a 0.51 mm platinum-sputtered, thin-film heater immersed in R-113 at saturation conditions under atmospheric pressure. Incipience superheat values just prior to these thermal excursions are large when using dielectric fluids and correspond to high wall temperatures, usually larger than those at the critical heat flux conditions. The main observations and conclusions of this study are given below.

(1) The incipience superheat excursion, under the conditions of this study was highly non-repeatable and, therefore, could not be described with single-sample measurements. The data is best presented in statistical form.

(2) Superheat levels of 24.0 ~ 38.9°C at incipience were measured for drawn chromel wires—corresponding embryonic bubble radii of 0.10 ~ 0.23 μ m were computed. The thin-film heater (platinum sputtered onto quartz) data showed incipience superheats of 49.1 ~ 72.5°C—embryonic bubble radii of 0.023 ~ 0.062 μ m were computed from this data. The higher superheat values measured on the thin-film heater (higher than those measured on the wire) are presumed to result from the absence of large cavities (>0.1 μ m) capable of entrapping bubble nuclei for incipience.

(3) Superheat excursions at the onset of nucleate boiling were strongly dependent upon the values of wall superheat at the beginning of the heat-up phase of the cycle (and the end of the cool-down phase of the previous cycle). This behavior is believed to be peculiar to low-wetting-angle fluids where the minimum radius of the incipience bubble embryo, within

the cavity, establishes the wall superheat or heat flux required for incipience. Thus, the minimum superheat between cycles establishes the superheat required for incipience.

(4) When the wall temperature exceeded 100°C, fouling deposits appeared. These deposits, presumed to be due to decomposition of the R-113, were shown to affect the nucleate boiling curve slightly, but not the incipience superheat values.

(5) The tests with large steps in heat flux showed increases in superheat excursion values (at the same probability) of as much as 20% over those of the small, incremental heat flux tests. The probability curves for boiling incipience are, apparently, dependent on how the heater is powered. These tests and the tests with small, incremental steps in heat flux seem to bracket the range of incipience performance attributable to the heat-up history.

Acknowledgement—This study was supported by a grant from the Commercial Chemicals Division of the 3M Company. The program monitors were R. D. Danielson, J. Githens and D. E. Maddox. Additional support was provided by the AMOCO foundation and by an AT&T equipment grant.

REFERENCES

1. S. Oktay, R. Hannemann and A. Bar-Cohen, High heat from a small package, *Mech. Engng* 36–42 (March 1986).
2. A. O. Greene and J. C. Wightman, Cooling electronic equipment by direct evaporation of liquid refrigerant, Air Material Command Rept PB 136065, Wright-Patterson Air Force Base, Fairborn, Ohio (1948).
3. A. E. Bergles, A. Bar-Cohen, P. J. Marto and K. P. Moran, Two phase liquid cooling, *NSF Workshop Proc. on Research Needs in Electronic Cooling*, pp. 26–51 (1986).
4. A. Bar-Cohen and T. W. Simon, Wall superheat excursions in the boiling incipience of dielectric fluids, *Heat Transfer Engng* 9(3), 19–31 (1988).
5. J. Lyman, Supercomputers demand innovation in packing and cooling, *Electronics* 136–143 (September 1982).
6. C. Corty and A. S. Foust, Surface variables in nucleate boiling, *Chem. Engng Prog. Symp. Ser. No. 51* 17, 1–12 (1955).
7. S. G. Bankoff, A. J. Hajjar and B. B. McGlothin, Jr., On the nature and location of bubble nuclei in boiling from surfaces, *J. Appl. Phys.* 29(12), 1739–1741 (1958).
8. R. D. Danielson, L. Tousignant and A. Bar-Cohen, Saturated pool boiling characteristics of commercially available perfluorinated inert liquid, *Proc. ASME/JSME Thermal Engng Joint Conf.*, Vol. 3, pp. 419–430 (1987).
9. P. J. Berenson, Experiments on pool-boiling heat transfer, *Int. J. Heat Mass Transfer* 5, 985–999 (1962).
10. S. K. R. Chowdhury and R. H. S. Winterton, Surface effects in pool boiling, *Int. J. Heat Mass Transfer* 28, 1881–1889 (1985).
11. Y. Kozawa, T. Inoue and K. Okuyama, Enhancement of bubble formation and heat removal in transient boiling, *Proc. 8th Int. Heat Transfer Conf.*, Vol. 4, pp. 2007–2212 (1986).
12. J. E. S. Venart, A. C. M. Sousa and D. S. Jung, Nucleate and film boiling heat transfer in R-11: the effects of enhanced surfaces and inclination, *Proc. 8th Int. Heat Transfer Conf.*, Vol. 4, pp. 2019–2024 (1986).
13. P. Griffith and J. D. Wallis, The role of surface con-

- ditions in nucleate boiling, *Chem. Engng Prog. Symp. Ser. No. 30* **56**, 49–63 (1959).
14. W. M. Marsh and I. Mudawwar, Effect of surface tension and contact angle on sensible heating and boiling incipience in dielectric falling film, *ASME Nat. Heat Transfer Conf. Proc.*, HTD-Vol. 96, pp. 543–550 (1988).
 15. J. J. Lorenz, B. B. Mikic and W. M. Rohsenow, The effect of surface condition on boiling characteristics, *Proc. 5th Int. Heat Transfer Conf.*, Vol. 4, B2.1, pp. 35–39 (1974).
 16. W. Tong, A. Bar-Cohen, T. W. Simon and S. M. You, Contact angle effects on boiling incipience of highly-wetting liquids, *Int. J. Heat Mass Transfer* **33**, 91–103 (1990).
 17. J. H. Lienhard, Corresponding state correlation for the spinoidal and homogeneous nucleation limits, *J. Heat Transfer* **104**, 379–381 (1982).
 18. S. J. Kline and F. A. McClintock, Describing uncertainties in single-sample experiments, *Mech. Engng* **75**, 3–8 (1953).
 19. T. H. Kuehn and R. J. Goldstein, Correlating equations for natural convection heat transfer between horizontal circular cylinder, *Int. J. Heat Mass Transfer* **19**, 1127–1134 (1976).
 20. S. Liaw and V. K. Dhir, Effect of surface wettability on boiling heat transfer from a vertical surface, *Proc. 8th Int. Heat Transfer Conf.*, Vol. 4, pp. 2031–2036 (1986).
 21. A. M. Schwartz and S. B. Tejada, Studies of dynamic contact angles on solids, *J. Colloid Interface Sci.* **38**(2), 359–375 (1972).
 22. W. M. Rohsenow, Boiling. In *Handbook of Heat Transfer* (Edited by W. M. Rohsenow and J. P. Hartnett), Section 13. McGraw-Hill, New York (1985).
 23. K. Akagawa, T. Sakaguchi and T. Fujii, Influence of fouling on boiling heat transfer to organic coolants, *Proc. 5th Int. Heat Transfer Conf.*, Vol. 4, B1.6, pp. 25–29 (1974).
 24. S. Yilmaz and J. W. Westwater, Effect of velocity on heat transfer to boiling Freon-113, *J. Heat Transfer* **102**, 26–31 (1980).
 25. L. Nghiem, H. Merte, E. R. F. Winter and H. Beer, Prediction of transient inception of boiling in terms of a heterogeneous nucleation theory, ASME Paper 80-HT-113 (1980).
 26. A. E. Bergles, N. Bakhru and J. W. Shires, Jr., Cooling of high power-density computer components, Engng Project Laboratory Rept 70712-60, MIT, Cambridge, Massachusetts (1968).
 27. J. Seeley and R. Chu, *Micro-electronic Heat Transfer*. Marcell–Dekker, New York (1972).
 28. R. W. Murphy and A. E. Bergles, Subcooled flow boiling of fluorocarbons—hysteresis and dissolved gas effects, *Proc. 1972 Heat Transfer and Fluid Mechanics Inst.*, pp. 400–416. Stanford University Press, Stanford, California (1972).
 29. M. D. Reeber and R. G. Frieser, Heat transfer of modified silicon surfaces, *IEEE Trans. CHMT-3*(3), 387–391 (1980).
 30. S. Oktay, Departure from natural convection (DNC) in low-temperature boiling heat transfer encountered in cooling micro-electronic LSI devices, *Proc. 7th Int. Heat Transfer Conf.*, Vol. 4, pp. 113–118 (1982).
 31. K. P. Moran, S. Oktay, L. Buller and G. Kerjilian, Cooling concept for IBM electronic packages, *IEPS Proc.* 120–140 (1982).
 32. P. J. Giarrantano, Transient boiling heat transfer from two different heat sources: small diameter wire and thin film flat surface on a quartz substrate, *Int. J. Heat Mass Transfer* **27**, 1311–1318 (1984).
 33. K. Ogiso, Recent trends in electronic equipment cooling, Paper J-6, NSF U.S./Japan Heat Transfer Joint Seminar, San Diego, California (1985).
 34. K. R. Samant and T. W. Simon, Heat transfer from a small high-heat-flux patch to a subcooled turbulent flow, *J. Heat Transfer* **111**(4), 1053–1059 (1989).

ETUDE EXPERIMENTALE DU DEBUT D'EBULLITION NUCLEEE AVEC UN FLUIDE DIELECTRIQUE TRES MOUILLANT (R-113)

Résumé—Des expériences sur le transfert de chaleur par ébullition en réservoir de R-113 à 1 atm sont conduites pour étudier des anomalies associées à l'initiation de l'ébullition à partir de fil de chromel de 0,13 mm de diamètre et d'un chauffoir à film mince en platine, de 0,51 mm de diamètre. Les valeurs de surchauffe de paroi allant jusqu'à 73°C à l'initiation et des larges variations d'un cas à l'autre sont observées. On recommande la présentation des résultats de surchauffe à l'apparition par des distributions de probabilité. On observe l'influence minimale correspondante de la paroi. Des tests avec des grands changements échelons des flux thermiques, utilisent un chauffoir cylindrique à film mince, indiquant des accroissements de la surchauffe à l'apparition d'à peu près 20% sur des tests avec des suites d'échelons incrémentiels de flux thermiques jusqu'au même niveau de flux thermique.

EXPERIMENTELLE UNTERSUCHUNG DES BEGINNS DES BLASENSIEDENS IN EINEM STARK BENETZENDEN DIELEKTRISCHEN FLUID (R-113)

Zusammenfassung—Es werden Experimente zum Wärmeübergang beim Behältersieden von gesättigtem R-113 bei Atmosphärendruck zur Untersuchung von Anomalien durchgeführt, die mit dem Siedebeginn verbunden sind. Es werden 0,13 mm dicke Drähte aus Chromel und 0,51 mm dicke Dünnschicht-Heizelemente aus Platin verwendet. Es wurden Wandüberhitzungen bis zu 73°C und eine weite Streubreite (mehr als 20°C) in den Wandüberhitzungen bei Siedebeginn von Fall zu Fall beobachtet—für nominell identische Zustände. Deshalb wird die Darstellung der Ergebnisse in Form von Wahrscheinlichkeitsverteilungen vorgeschlagen. Der signifikante Einfluß der minimalen Wärmestromdichte und der zugehörigen minimalen Wandüberhitzung (nach der Abkühlungsphase einer Meßreihe und dem Beginn der folgenden Meßreihe) auf den Siedebeginn wurde beobachtet. Versuche mit großen Abstufungen der Wärmestromdichte unter Verwendung eines zylindrischen Dünnschicht-Heizelements zeigten eine Zunahme der Wandüberhitzung bei Siedebeginn von mehr als 20% gegenüber Versuchen mit enggestufter Erhöhung der Wärmestromdichte bis zum selben Niveau.

**ЭКСПЕРИМЕНТАЛЬНОЕ ИССЛЕДОВАНИЕ ЗАРОЖДЕНИЯ ПУЗЫРЬКОВОГО
КИПЕНИЯ ВЫСОКОСМАЧИВАЮЩЕЙ ДИЭЛЕКТРИЧЕСКОЙ ЖИДКОСТИ (R-113)**

Аннотация—Для изучения аномалий, связанных с началом кипения, проведено экспериментальное исследование теплопереноса в условиях кипения в большом объеме насыщенной жидкости R-113 при давлении, равном 1 атм., с использованием горизонтальных хромелевых проволочек диаметром 0,13 мм и платинового тонкопленочного нагревателя диаметром 0,51 мм. Для почти идентичных случаев получено, что величины перегрева стенки при зарождении кипения составляют до 73°C и наблюдаются значительные их колебания (более чем на 20°C). В этой связи такие результаты предложено выражать в виде распределения вероятности. Отмечено существенное влияние минимального теплового потока и соответствующего минимального перегрева стенок (на стыке двух опытов) на различие в величинах перегрева. В экспериментах с большими скачкообразными изменениями теплового потока, проведенных на тонкопленочном цилиндрическом нагревателе, отмечено превышение этих величин на 20% по сравнению с опытами, в которых происходит постепенное увеличение теплового потока до такого же его уровня.